Comparison of Transient and Successful Fusion Pores Connecting Influenza Hemagglutinin Expressing Cells to Planar Membranes

GRIGORY B. MELIKYAN, WALTER D. NILES, VLADIMIR A. RATINOV,* MILOSH KARHANEK, JOSHUA ZIMMERBERG,* and FREDRIC S. COHEN

From the Department of Molecular Biophysics and Physiology, Rush Medical College, Chicago, Illinois 60612; and *Laboratory of Theoretical and Physical Biology, National Institute of Child Health and Human Development, Bethesda, Maryland 20892

ABSTRACT Time-resolved admittance measurements were used to investigate the evolution of fusion pores formed between cells expressing influenza virus hemagglutinin (HA) and planar bilayer membranes. The majority of fusion pores opened in a stepwise fashion to semistable conductance levels of several nS. About 20% of the pores had measurable rise times to nS conductances; some of these opened to conductances of ~500 pS where they briefly lingered before opening further to semistable conductances. The fall times of closing were statistically similar to the rise times of opening. All fusion pores exhibited semistable values of conductance, varying from ~2–20 nS; they would then either close or fully open to conductances on the order of 1 μS. The majority of pores closed; ~10% fully opened. Once within the semistable stage, all fusion pores, even those that eventually closed, tended to grow. Statistically, however, before closing, transient fusion pores ceased to grow and reversed their conductance pattern: conductances decreased with a measurable time course until a final drop to closure. In contrast, pore enlargement to the fully open state tended to occur from the largest conductance values attained during a pore's semistable stage. This final enlargement was characterized by a stepwise increase in conductance. The density of HA on the cell surface did not strongly affect pore dynamics. But increased proteolytic treatment of cell surfaces did lead to faster growth within the semistable range. Transient pores and pores that fully opened had indistinguishable initial conductances and statistically identical time courses of early growth, suggesting they were the same upon formation. We suggest that transient and fully open pores evolved from common structures with stochastic factors determining their fate.

INTRODUCTION

The fusion pore is the portion of two fusing membranes that establishes the continuity of formerly distinct bilayers, through which the contents of previously sepa-

Address correspondence to Dr. Fredric S. Cohen, Department of Molecular Biophysics and Physiology, 1653 West Congress Parkway, Chicago, IL 60612.

J. GEN. PHYSIOL. © The Rockefeller University Press · 0022-1295/95/11/803/17 $2.00
Volume 106 November 1995 803–819

rated aqueous compartments mix (White, 1992; Zimmerberg, Vogel, and Chernomordik, 1993). Once formed, pore sizes, measured as conductances, progress in stages: pores quickly enlarge to within a range of sizes where they remain for variable times, referred to as semistable conductances. Pores then either close (termed transient pores) or rapidly enlarge to their final sizes (fully open pores). This staged growth has been shown for mast cell exocytotic secretion (Monck and Fernandez, 1992; Nanavati, Markin, Oberhauser, and Fernandez, 1992; Curran, Cohen, Chandler, Munson, and Zimmerberg, 1993), baculovirus-mediated cell–cell fusion (Plonsky and Zimmerberg, 1994), and for influenza hemagglutinin (HA) mediated fusion of cells to erythrocytes (Spruce, Iwata, White, and Almers, 1989; Spruce, Iwata, and Almers, 1991; Tse, Iwata, and Almers, 1993; Zimmerberg, Blumenthal, Sarkar, Curran, and Morris, 1994) and to planar phospholipid bilayers (Melikyan, Niles, Peeples, and Cohen, 1993*a*; Melikyan, Niles, and Cohen, 1993*b*). In viral infection of cells, release of large (~50 nm) viral nucleocapsids can only occur through fully enlarged pores. We therefore refer to semistable pores that will eventually fully enlarge as "successful."

Staged growth of fusion pores appears to be universal, suggesting that a global property common to all fusion systems is the basis of the phenomenon. In this paper, the growth of fusion pores connecting HA-expressing cells to planar membranes has been followed using time-resolved admittance measurements. We compare the early conductance trajectories of pores that eventually closed to those that fully opened, to determine whether early behavior could predict their fate. We found that the conductances of the initial pores and their increases soon after formation were independent of whether they eventually fully opened or closed. We conjecture that pores that subsequently close and pores that eventually dilate fully are initially the same structures, and thus their fates are controlled by stochastic processes.

MATERIALS AND METHODS

General Procedures

Cell culturing, treatment of cells, and planar bilayer formation were exactly as described in the companion paper (Melikyan, Niles, and Cohen, 1995). HAb2 and GP4f cell lines, transfected 3T3 fibroblasts (White, Helenius, and Gething, 1982; Sambrook, Rodgers, White, and Gething, 1985), were used. Both express the HA of the A/Japan/305/57 strain influenza virus, but HAb2 expresses HA at higher surface density (Ellens, Bentz, Mason, Zhang, and White, 1990). HAb2 and GP4f cells were treated in various manners, symbolized by *X/Y* where *X* marks whether the activation of HA0 by trypsin was full (*F*), extensive (*E*) or low (*L*) and *Y* refers to the enzymatic treatment of the cell surfaces. Surfaces were either treated with high concentrations of trypsin (*T*), chymotrypsin (*C*), hyaluronidase/collagenase (*H*), or untreated (*U*). For purposes of notation, chymotrypsin-treated HAb2 cells with HA0 extensively cleaved by a 12-min incubation with a low concentration (1 μg/ml) of trypsin, for example, are denoted E/C HAb2 cells. In fusion experiments, 15–25 HA expressing cells were layered upon voltage-clamped horizontal, ganglioside-containing (G_{D1a}/G_{T1b} 1:1 wt/wt), planar bilayers. Fusion was triggered by lowering the pH of the top, cell-containing, aqueous compartment.

Time Resolved Admittance Measurements

Cell-planar bilayer fusion was monitored by electrical admittance measurements as described (Melikyan et al., 1993*a*) but replacing an analogue lock-in amplifier with a software-based one (Joshi and Fernandez, 1988). A horizontal planar bilayer was voltage clamped with a custom-built current amplifier. A 100 Hz or 1 kHz sine wave voltage (1 V p-p) superimposed on a holding potential of +1 V (referred to the bottom, cell-free, *trans* compartment of the experimental chamber with the top solution grounded) was generated by a 486 class computer using a 12-bit D/A converter (model STB-16; Analogic Corp., Wakefield, MA) and applied to the command input of the current amplifier after 1:50 attenuation (i.e., 20 mV p-p was applied across the planar membrane). The output signal of the current amplifier was filtered with a four-pole Butterworth filter (model 3321; Krohn-Hite, Avon, MA) at 10 kHz and sampled with 16-bit resolution every 25 μs (STB-16; Analogic Corp.). The signals in-phase (Y_0) and 90 out-of-phase (Y_{90}) with respect to the applied voltage were calculated for each sine wave period and displayed on-line. Y_0 and Y_{90} currents were converted into their natural units of conductance (nS). Also, direct current conductance (Y_{dc}) was calculated and displayed simultaneously. Data were stored on hard disk and analyzed off-line.

We set the specific phase angle for admittance measurements by switching an 11-pF calibrated air-gap capacitor into and out of the circuit between the voltage clamp amplifier input and ground, with a reed relay (Coto, Providence, RI). The computer automatically adjusted the phase angle so that Y_0 did not change with changes in capacitance. We used this procedure to find the phase retardation introduced by the current amplifier and anti-aliasing filter ($\approx 20°$ at 1 kHz). The planar membrane in series with its low access resistance (20–30 kΩ) caused $<1°$ phase shift at 1 kHz and negligible shift at 100 Hz. Thus, our protocol of setting the phase angle, in effect, ignored the series resistance. In theory, for a 1 kHz sine wave, this caused a $<5\%$ error in the measured Y_0. In practice, small transient pores were observed with only Y_0 signals occurring (see below), without detectable Y_{90} signals, verifying the reliability of the measurement.

Data Analysis

Fusion was modeled by the simplified three element equivalent circuit (Fig. 1, *top*) consisting of the fusion pore conductance, g, in series with the parallel combination of cell conductance, G_c, and capacitance, C_c. g, G_c, and C_c, were calculated from changes in Y_0, Y_{90}, and Y_{dc} (Lindau and Neher, 1988; Pusch and Neher, 1988). This equivalent circuit was justified because the series resistance to the bilayer was stable and small, and the bilayer conductance (G_m) was on the order of 0.1 nS at the beginning of an experiment and could be neglected. The capacitance of the planar membrane, C_m, (typically 150–160 pF with the Teflon partition) was compensated with the capacitance cancellation circuitry of the current amplifier before triggering fusion. But C_m tended to drift slowly before and after the onset of fusion. We explicitly compensated the drift before fusion pore formation with the capacitance cancellation circuitry. Slow drift in capacitance between flickering fusion pores was digitally compensated off-line by low-pass filtering the baseline of each of the three admittance traces and subtracting them from their original records. The mean and variance of each corrected baseline was calculated before the first fusion pore opening. Three consecutive calculated points more than two standard deviations above the mean of a baseline were taken as true openings; pore closings were handled in an analogous fashion. For simplicity of notation, in the remainder of this paper, Y_0, Y_{90}, and Y_{dc} denote the deviations measured from baseline for each of the respective admittance components.

For a stimulating sine wave frequency, f, of 1 kHz, g was calculated at 1 ms/point using $g = Y_0$. We affirmed the time response of the planar bilayer system by checking that the rise times of open and shut transitions of VDAC (mitochondrial voltage-dependent anion channels) obtained from Y_0 were always within 1 ms for a 1 kHz sine wave. We took this time as instantaneous. g was deter-

mined soon after pore opening (denoted $g_{f,o}$ and $g_{s,o}$ for flickering and successful pores, respectively) and soon before flickering pores completely closed ($g_{f,c}$). To evaluate the early dynamics of pore conductance and to compare flickering and successful pores, $g_{f,o}$ and $g_{s,o}$ were determined at both 2 and 4 ms after opening for each cell treatment. In an analogous fashion, $g_{f,c}$ was measured 2 and 4 ms before flickering pores completely closed. Also, g was examined for the one half of the flickering pores that were still open at the median open time ($g_{f,m}$). Finally, the maximal conductance of each pore, whether transient ($g_{f,max}$) or successful ($g_{s,max}$), was determined. Values of g were plotted as cumulative distributions, obtained by rank ordering conductance values and normalizing their rank by the total number of measurements. Differences between conductance distributions (e.g., Fig. 7) were evaluated by the nonparametric Kolmogorov-Smirnov test.

RESULTS

Fusion Pore Conductances Calculated from a Three Element Equivalent Circuit

The addition of the cell to the planar membrane upon fusion was modeled by an equivalent circuit consisting of the fusion pore, g, in series with the parallel combi-

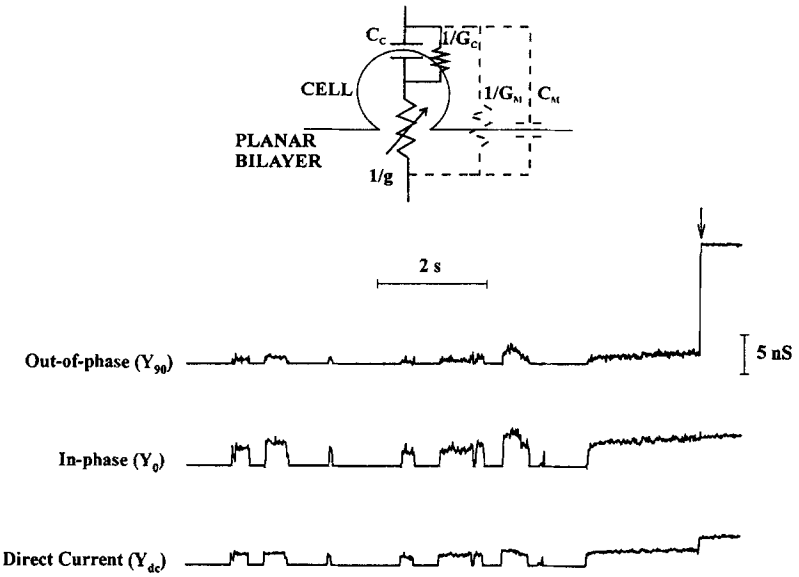

FIGURE 1. (*Top*) Equivalent three element circuit of the fusion pore connecting the cell to the planar bilayer. C_c and G_c are the cell membrane capacitance and conductance, respectively; g is the fusion pore conductance. The planar bilayer conductance, G_m, was neglected. The bilayer capacitance, C_m, was compensated by capacitance cancellation circuitry. (*Bottom*) Typical Y_{90}, Y_0 and Y_{dc} signals upon fusion of HAb2 cells to a ganglioside-containing planar bilayer. 19 F/T HAb2 cells were adhered to a voltage-clamped horizontal bilayer for 4–5 min at pH = 6.3. A 100-Hz sine wave (30 mV p-p) was superimposed on a 20 mV holding potential. Fusion was then triggered by acidifying the top solution by adding a concentrated isotonic succinate buffer (pH 4.9). The records start 107 s after acidification. The flickering seen as changes in the three traces were due to fusion pores opening and closing. For visual clarity, an experiment was chosen where the time was short from the first flicker to the abrupt jump in Y_{90} (*arrow*) associated with full enlargement of the fusion pore.

nation of the cell membrane conductance, G_c, and capacitance, C_c (Fig. 1, *top*). This three element circuit is formally equivalent to that for patch-clamped cells in the whole cell mode, wherein the resistance of the patch pipette is in series with the cell membrane. The circuit elements are obtained from the measured admittance components (Lindau and Neher, 1988; Pusch and Neher, 1988). Using notation where fusion pores substitute for pipettes, the equations are:

$$\begin{aligned} g &= a/b \\ G_c &= aY_{dc}/(b^2 + Y_{90}{}^2) \\ C_c &= a^2/(\omega Y_{90}[b^2 + Y_{90}{}^2]) \end{aligned} \tag{1}$$

where

$$a = Y_0{}^2 + Y_{90}{}^2 - Y_0 Y_{dc},\ b = Y_0 - Y_{dc}\,.$$

In whole cell patch clamp experiments, C_c increases upon fusion of granules to plasma membranes (Lindau and Neher, 1988). However, g is not calculated in whole cell experiments using the three-element circuit; such calculations are precluded by the high and variable series resistance of the patch pipette. Because of this problem, it has traditionally been assumed that G_c is constant and does not contribute to admittance changes (Zimmerberg, Curran, Cohen, and Brodwick,

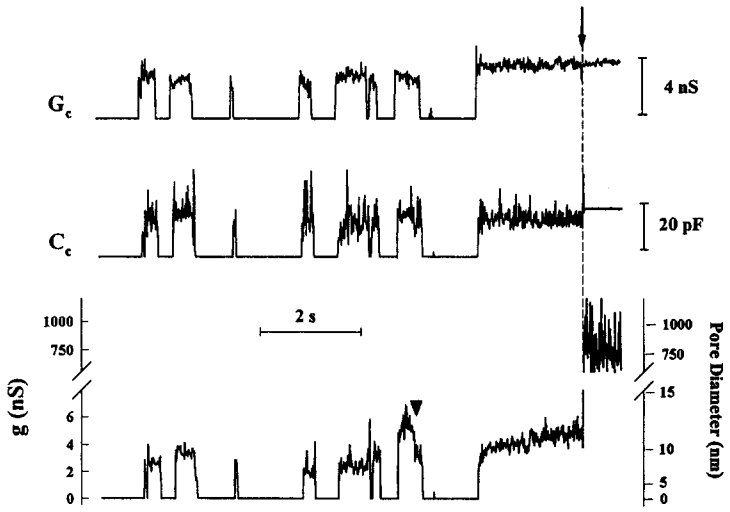

FIGURE 2. The fusion pore conductance, g, cell membrane conductance, G_c, and cell capacitance, C_c, for the experiment of Fig. 1, using the system of equations (Eq. 1). Fusion pores repetitively flickered to conductances of ~2–6 nS. Changes in conductance of open fusion pores (e.g., *arrowhead*) are not associated with changes in G_c and C_c. Also, the calculated values of G_c and C_c do not change when the fusion pore rapidly dilates (*arrow*) to a large conductance, ≈1,000 nS. Upon this dilation, the voltage drops entirely across the cell membrane and the signal-to-noise ratio of Y_{90} is increased; the variance of the calculated C_c becomes greatly reduced. The right-hand ordinate converts the pore conductance into approximate diameters, assuming a pore length of 15 nm and specific resistivity of solution of 100 Ω-cm.

1987). In the cell-bilayer fusion system, however, the resistance in series with the planar membrane is small and stable. Hence, any changes in G_c are explicitly accounted for by the three element circuit and do not contaminate evaluation of g. This is of practical consequence because G_c of HA-expressing cells tends to increase at low pH (Spruce et al., 1989). But the three element model is applicable only when contributions to changes in admittance from the planar bilayer are negligible or can be compensated (see Materials and Methods). In practice, the equivalent circuit is adequate if the planar membrane conductance, G_m, does not increase appreciably during the experiment.

Y_0, Y_{90}, and Y_{dc} changed in a stereotypic manner after triggering fusion by acidifying the solution bathing cells which were in contact with the planar membrane (Fig. 1). After acidification, there was an electrically quiescent stage followed by flickering in Y_0, corresponding to the opening and closing of fusion pores. Concomitant changes in Y_{90} were observed for low stimulating frequencies (e.g., 100 Hz, Fig. 1), but not at high frequencies (e.g., 1 kHz, Fig. 3).

The values of G_c, C_c, and g were calculated as a function of time from Eq. 1 for the experiment of Fig. 1, and are shown in Fig. 2. Whenever the pore closed, the cell was no longer electrically connected to the planar membrane and the absence of admittance signals resulted in G_c and C_c calculated as zero. The values of Y_0 and Y_{90} for open pores differed for each flicker: each flicker had its own pattern of open pore conductance, g. The fusion pore is dynamic and hence it would be expected that the calculated g should vary. However, the cell membrane is relatively static and hence the calculated G_c and C_c should remain constant during a flicker. These behaviors were observed. For example, there was a distinct decrease in g (marked by bold arrowhead) during the last flicker. But the calculated G_c and C_c remained constant. This argues for the quantitative reliability of parameters derived from the three element equivalent circuit. The present method is an improvement over the two element circuit that describes fusion as a fusion pore conductance, g, in series with the cell capacitance, C_c (Melikyan et al., 1993*a*).[1]

Our present calculations for fusion pore conductance depend on Y_{dc}. But discharge of cell resting potentials through fusion pores would contribute to dc current and hence to Y_{dc}, a contribution not accounted for in the present technique (Lindau and Neher, 1988). As shown below we determined that ignoring cell potentials did not affect the calculated circuit elements. This was probably due to the fact that nonspecific leakages, which would shunt any ion-selective reversal potentials, dominated the cell conductances, usually ~2–4 nS at low pH. These leakages resulted from removing cells from culture dishes for fusion experiments. While adhered to dishes, virtually all cells excluded trypan blue. After removal, only ≈50% of the cells excluded trypan blue. Hence, cell resting potentials were probably close

1. In control experiments with VDAC, open-channel conductances obtained from Y_0 were constant and did not fluctuate. This establishes that the fluctuations in fusion pore conductances were due to changes in fusion pore sizes, and not due to the technique of measurement.

to zero and ignoring them did not negate the validity of our calculations. This presumption was corroborated by the fact that the calculated G_c did not change even after full pore dilation (Fig. 2, *arrow*): dilation led to a rapid dialysis of cells by the *trans* solution (Melikyan et al., 1993*a*) which would eliminate nonzero resting potentials.

We performed control experiments to explicitly investigate whether resting potentials of HAb2 cells affected our calculations. We simultaneously applied two stimulating sine waves, typically at frequencies of 100 and 1,000 Hz, in addition to a dc voltage and measured Y_0 and Y_{90} at each frequency as well as Y_{dc}. The three circuit elements can be determined by employing stimulating voltages of any two frequencies. Routinely we used a single non-zero and a zero (dc) frequency voltage. Whereas a discharge of a resting potential through g would contribute to Y_{dc}, it would not contribute to admittance components measured at other frequencies (Rohlicek and Rohlicek, 1993; Donnelly, 1994). Thus, fusion pore conductances calculated from two pairs of Y_0 and Y_{90} do not depend on the cell resting potentials. The calculated values of g using pairs of Y_0, Y_{90} were identical to the values calculated from Y_{dc} and a single frequency-pair of Y_0, Y_{90} (data not shown). Thus, in practice, the circuit elements are properly calculated when assuming a zero voltage resting potential.

Using a 1 kHz stimulating sine wave, typical for achieving high time resolution, a large change was observable in Y_0 with no change in Y_{90} when a small pore opened. This change occurred because virtually the entire applied voltage dropped across the resistance of the small pore with negligible voltage across the large cell membrane whose capacitive admittance equaled $\omega C_c \approx 100$ nS. Despite the absence of a detectable Y_{90} signal upon opening of small pores, g and G_c could be calculated, provided that $Y_0 > Y_{dc}$. In this case, $Y_0 \approx g$ and $G_c = Y_0 Y_{dc}/(Y_0 - Y_{dc})$; C_c was indeterminate. These simplified equations are valid for fusion pores up to 25 nS (for f = 1 kHz, C_c = 20 pF); for larger pores Y_{90} signals occur and the full set of equations (Eq. 1) must be used. As fusion pore conductances were usually below 25 nS before the pore abruptly expanded into a large terminal stage (Fig. 3), Y_0 was a reliable estimator of g in the great majority of our experiments conducted at high frequency. Our signal-to-noise ratio and the cell's nonzero G_c precluded detecting pore conductances smaller than ~0.3 nS at high time resolution.

When a fusion pore dilated toward its final large conductance in the T stage ($\approx$1,000 nS) Y_{90} increased in a stepwise fashion (Figs. 1 and 3), because the voltage drop switched from across the pore to across the capacitance of the fusing cell membrane. This switching was also marked by a decrease in Y_0 at a high stimulating frequency (Fig. 3), as quantitatively described by the equations (Eq. 1) for the three element equivalent circuit. Y_0 did not fully return to baseline because a small fraction of the applied voltage still dropped across a 1,000 nS pore and G_c was not necessarily zero. The major contribution to the final Y_0 signal (Fig. 3) was attributable to the voltage drop across the fusion pore because Y_{dc} was small compared to Y_0. However, with a low stimulating frequency, the Y_0 trace did not necessarily decay toward the original baseline. The voltage dropped entirely across the cell membrane after the pore fully enlarged and the residual $Y_0 \approx Y_{dc} \approx G_c$ (Fig. 1).

Flickering Pores Enlarge Rapidly upon Opening and Contract Quickly Just Before Full Closure

Pores instantaneously opened to conductances of 1–4 nS in ~80% of the cases (Figs. 4, *A* and *B*), and more slowly for 20% (Figs. 4, *C–F*). About 5% of the transi-

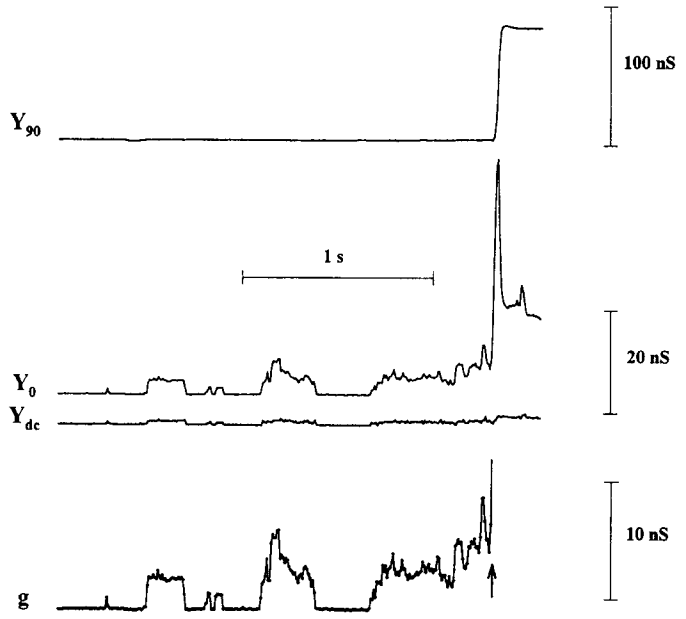

FIGURE 3. Measurement of cell-planar bilayer fusion monitored at high frequency. A stimulating sine wave voltage (1 kHz, 20 mV p-p) was superimposed on a 20-mV holding potential. 17 cells (F/T HAb2) were brought into contact with a horizontal planar bilayer. After 4 min of contact, fusion was triggered by injecting concentrated succinic acid (pH 4.9). Record is shown 82 s after acidification. The Y_{90}, Y_0, and Y_{dc} signals are typical of fusion pore formation and evolution. The Y_{90} signal did not change upon pore flickering because of the large cell admittance. But it increased in a stepwise fashion when the pore fully enlarged. The lowermost trace shows the fusion pore conductance calculated for a three-element equivalent circuit (see Materials and Methods). Calculated points were decimated (to 10 ms/pt) for visual clarity. In this record, five sequential transient pore openings are shown. Then a pore remained securely open before a fast dilation to a large value of conductance (*arrow up*). This enlargement is reflected in the stepwise increase of Y_{90} and decrease of Y_0. Y_0 did not fully return to baseline; the deviation yields the final large, but finite, pore conductance, usually ~1 μS (not shown).

tions clearly paused at conductances of approximately 0.5–0.6 nS (Figs. 4, *E* and *F*) before further enlarging to conductances of 1–4 nS. The time course of closings statistically resembled those of openings. The majority of the closings were instantaneous (Figs. 5, *A* and *B*). Some closings exhibited noninstantaneous, smoothly decaying falls in conductance (Figs. 5, *C* and *D*). A small percentage of the pores fell to a small conductance, again ~0.5 nS (Figs. 5, *E* and *F*), where they dwelled before fully closing.

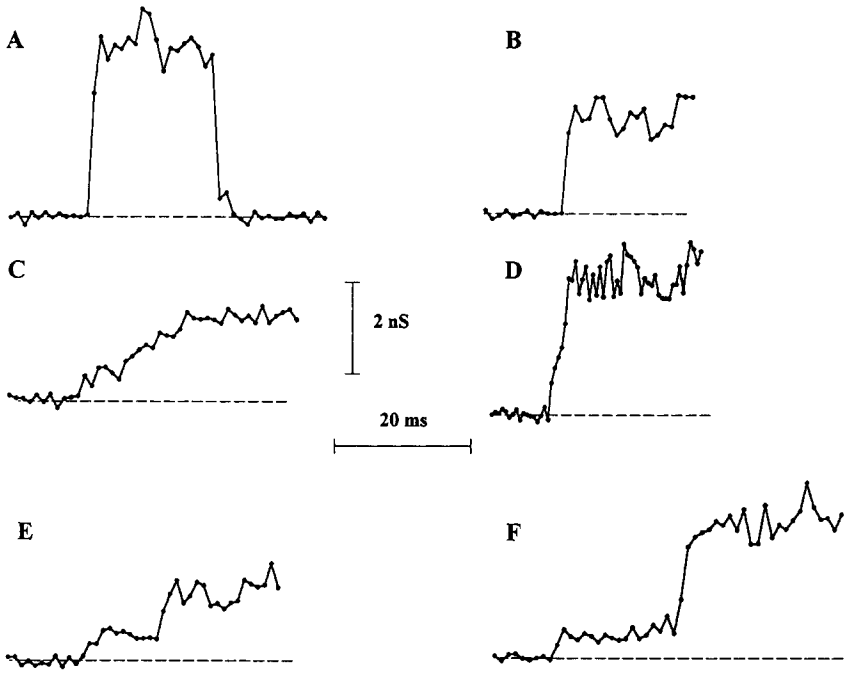

FIGURE 4. Different paths for early enlargement of fusion pores. *A* and *B* show pores that "instantaneously" opened to semistable values of conductances on the order of a few nS. *C* and *D* illustrate pores that increased to semistable conductances with slower rise times. *E* and *F* show pores that lingered at intermediate conductances of ~0.5 nS before further dilating to semistable conductance values. These fusion pore conductances, obtained from experiments performed with a 1 kHz stimulating sine wave, were estimated directly from the Y_0 signal.

The tendency of pores to grow within the first few milliseconds after opening or to shrink in the last few milliseconds before closing is demonstrated by plotting the cumulative distributions of pore conductances at times a few ms apart soon after opening ($g_{f,o}$; Fig. 6 *A*) and just before closing ($g_{f,c}$; Fig. 6 *B*). The conductances 2 ms (*thick lines*) after opening (Fig. 6 *A*) and before closing (Fig. 6 *B*) were statistically smaller than at 4 ms (*thin lines*) after opening and 4 ms before closing, respectively. The $g_{f,o}$ and $g_{f,c}$ distributions were identical to each other (compared at both 2 and 4 ms after pore opening and before closure, respectively). While the time courses of increases after opening and decreases before closing were comparable on the population level, instantaneous or noninstantaneous rises to the nS range of conductances did not correlate with fall times from these conductances to full closure on the level of individual transient pores. Thus, the profile of the rises in conductance of an individual flickering pore did not provide information about its closing conductance profile. Because intermediate small conductances were resolved for only a fraction of events, the initial $g_{f,o}$ (Fig. 6 *A*) and final $g_{c,o}$ (Fig. 6 *B*) distributions are dominated by conductances larger than 1 nS. But, even flickering pores that opened (or closed) instantaneously tended to exhibit fast increases (or decreases) in conductance.

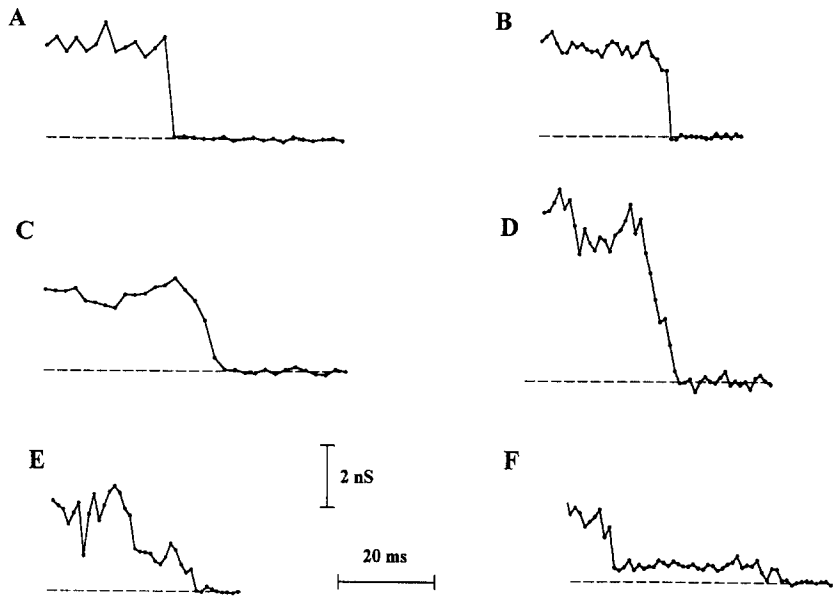

FIGURE 5. Pores close from semistable conductance levels in varied manners. (*A* and *B*) Instantaneous, within 1 ms, closings. (*C* and *D*) Gradual conductance decreases over several ms. (*E* and *F*) Pausing of pores at an intermediate conductance, ~0.5 nS, before complete closure.

Transient Pores Slowly Enlarge, Then Contract Before Fully Closing

We statistically characterized the conductance trajectories of transient pores after the early fast enlargement: we calculated fusion pore conductances at the median open time of flickering pores, $g_{f,m}$, and compared these distributions to $g_{f,o}$ and $g_{f,c}$. The median time was obtained from the open time distribution for each treatment

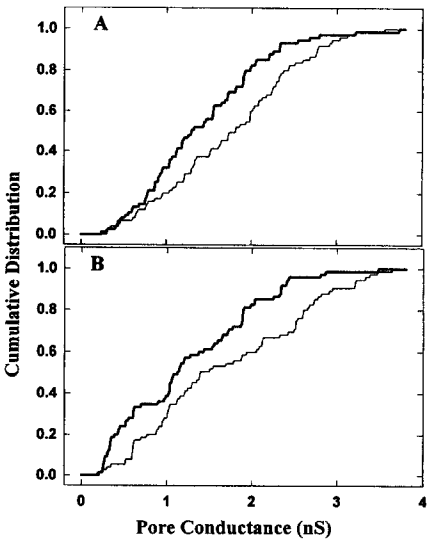

FIGURE 6. Cumulative probability distributions of transient fusion pore conductances after opening, $g_{f,o}$, (*A*) and before closing, $g_{f,c}$, (*B*) measured for E/C HAb2 cells. Bold lines correspond to pore conductance distributions measured 2 ms after opening or 2 ms before closing. Thin lines represent the distributions 4 ms after opening or before closing. The 4-ms distributions are shifted to larger conductances ($p < 0.05$). This reflects the fast enlargement soon after pore formation and fast contraction just before complete closure. $N = 75$.

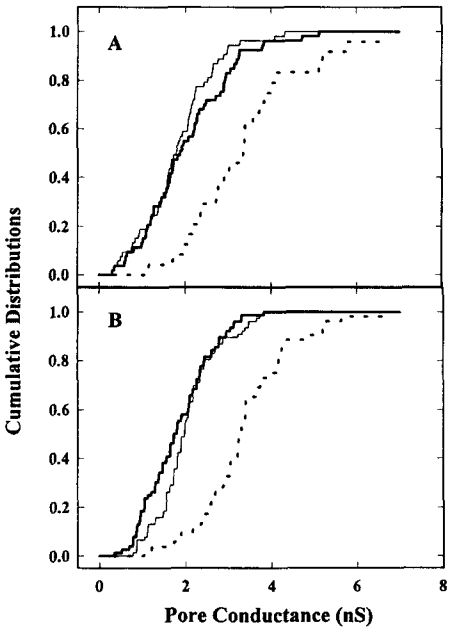

FIGURE 7. Dependence of open transient fusion pore conductances on HA surface density. (*A*) Cumulative distributions of pore conductances for E/U HAb2 cells (medium HA density): $g_{f,o}$ (measured 4 ms after opening, *thick solid line*); $g_{f,m}$ (measured at the median open time, *dotted line*); $g_{f,c}$ (4 ms before final closure, *thin solid line*). The distributions of conductances of pores upon opening were statistically identical to the conductances from which pores closed ($p > 0.1$). Slow enlargement followed by contraction of pores is shown by the shift of $g_{f,m}$ ($N = 24$) to larger conductances than $g_{f,o}$ and $g_{f,c}$ ($p < 0.005$, $N = 53$). (*B*) Cumulative distributions of pore conductances for L/U HAb2 cells (low HA density). $g_{f,o}$ (*thick solid line*) and $g_{f,c}$ (*thin solid line*) distributions were identical ($p > 0.1$, $N = 76$) and statistically smaller than $g_{f,m}$ ($p < 0.005$, $N = 52$) shown as a dotted curve. $g_{f,o}$ and $g_{f,c}$ measured 2 ms after opening and before full closing, respectively, were statistically identical. Because pore conductances increased between 2 and 4 ms after opening and decreased between 4 and 2 ms before closing (Fig. 6) the difference between $g_{f,o}$ and $g_{f,c}$ measured at the 2-ms points and $g_{f,m}$ was greater than for the distributions shown.

protocol (Melikyan et al., 1995). $g_{f,o}$ (*thick solid line*, 4 ms after opening), $g_{f,m}$ (*dotted line*), and $g_{f,c}$ (*thin solid line*, 4 ms before closing) are shown as cumulative distributions for HAb2 cells with an extensive (E/U; Fig. 7 *A*) and a low level of HA0-cleavage (L/U; Fig. 7 *B*) by trypsin. Whereas the $g_{f,o}$ and $g_{f,c}$ distributions were identical for all cell treatment protocols, the $g_{f,m}$ distribution was statistically larger than the other two. Thus, the following picture of pore behavior emerges (Fig. 8): pores tend to immediately expand after formation. After a few ms of fast enlargement they reach semistable conductances, continuing to grow, but at a slower rate. Statistically, they do not immediately close from the enlarged conductance values. If they

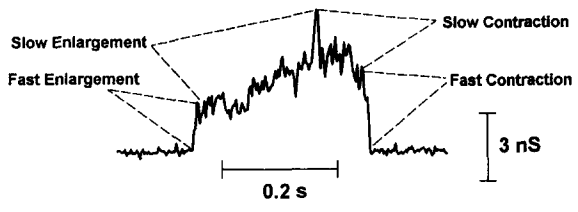

FIGURE 8. Stereotypic enlargement and contraction of a transient fusion pore. Upon formation, the fusion pore enlarges within a few milliseconds (fast enlargement) to a semistable conductance level. The pore continues to enlarge but at a slower rate (slow enlargement). The pore then reverses its growth and contracts slowly (slow contraction) before the fast contraction to full closure.

have expanded significantly, they tend to slowly contract back to conductances comparable to those at formation before the fast final closing.

The density of active HA did not affect the slow growth, the initial conductances, nor the lifetimes of transient open pores (Melikyan et al., 1995). In contrast, pore growth was affected by the manner in which cell surfaces were proteolytically treated, treatments that altered the nature of surfaces but not the density of active HA. While pores opened to and closed from conductances that did not appreciably vary with proteolytic treatment, the slow pore enlargement was delayed when cell surfaces were not treated: while the $g_{f,m}$ distributions for HAb2 cells did not change with proteolytic treatment ($p > 0.05$, not shown), the median pore open times did depend on treatment (Melikyan et al., 1995). E/U and L/U cells exhibited the longest median open times, ~600 ms. For proteolytically treated cell surfaces, median open times were between 100–200 ms (≈200 ms for F/T HAb2 cells, ≈100 ms for E/C and E/H HAb2 cells). It follows that the rates of pore growth were slower for E/U and L/U HAb2 cells than for proteolytically treated cells. This provides further evidence for our previous conclusion that cell proteolytic treatment leads to faster open pore dynamics (Melikyan et al., 1995). Also, while pore conductances were greater at 200 ms than at opening (i.e., $g_{f,m} > g_{f,o}$) for treated cells, for untreated cells they were the same (i.e., $g_{200\ ms} = g_{f,o}$, $p > 0.05$). Thus, with untreated cells, pores were inclined to enlarge somewhere between 200 and 600 ms (their median open time) after formation.

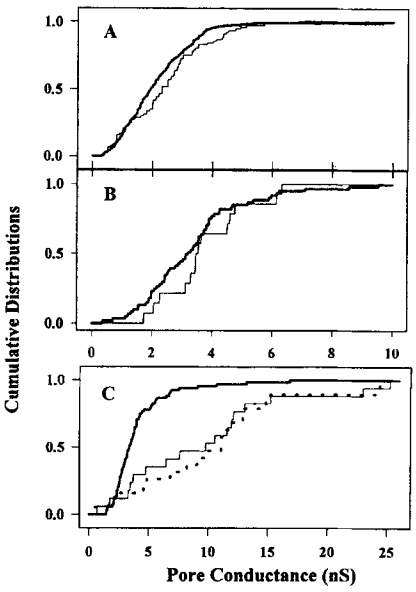

FIGURE 9. Comparison of conductance trajectories of transient and successful pores. (*A*) Initial (2 ms) conductance distributions for transient (*thick solid line*) and successful (*thin solid line*) pores. Transient and successful open pores exhibited the same conductances upon formation ($p > 0.1$). Data for all treatment protocols of HAb2 cells were pooled together ($N = 386$ for transient pores and $N = 77$ for successful pores). (*B*) Conductance distributions of transient and successful fusion pores at the median open time of transient fusion pores from F/T HAb2 cells. $g_{f,m}$ (*thick line*) and $g_{s,m}$ (*thin line*) were statistically indistinguishable ($p > 0.1$). (*C*) Maximal conductances for transient (*thick solid line*) and successful open (*thin solid line*) pores between F/T HAb2 cells and bilayer. Successful pores exhibited rapid, usually too fast to be measured, increases from semistable conductances to their fully open μS values. To be certain that digitized points of transition conductances into fully open μS conductance pores were not assigned as maxima of the semistable conductances of successful pores, the last two digitized points of the semistable conductance stage were excluded. Pores fully dilated from the maximal semistable conductances—the distribution of semistable conductances of successful pores from which fast dilation to fully open pores occurred ($g_{S\text{-}T}$, *dotted line*) was not statistically different from the maximal conductances ($p > 0.1$; $N = 68$ for transient and $N = 19$ for securely open pores).

Early Conductances of Transient and Successful Open Pores Do Not Differ

We addressed whether transient pores and successful pores that fully opened derived from similar structures by comparing their initial conductance distributions and their increases over time. The distributions of initial conductances of transient, $g_{f,o}$ (Fig. 9 *A, thick line*) and of successful pores, $g_{s,o}$ (*thin line*) were not statistically different when data from the various cell treatment protocols were pooled. There was also no difference in distributions between flickering and successful pores for each individual treatment protocol ($p > 0.1$, data not shown). Nor did the mean $g_{f,o}$ for flickering pores within an individual experiment show differences from the initial conductance for the successful pore from the same experiment ($p > 0.1$). In short, comparing $g_{f,o}$, for transient, and $g_{s,o}$, for pores that fully open, in various manners leads to the same conclusion: that flickering and successful pores appear with the same initial distributions of conductance. In addition to opening with the same conductances, flickering and successful pores enlarged at similar rates: the distribution of conductances measured at the median open time of transient pores were the same for transient, $g_{f,m}$ (Fig. 9 *B, solid line*) and successful, $g_{s,m}$ (Fig. 9 *B, thin line*), pores. The identity of conductances and early growth of transient and successful pores is consistent with the idea that these pores have the same structure upon formation and that stochastic processes determine whether they close or fully open.

Both flickering and successful pores exhibited semistable conductances. For the cell-planar bilayer system, these conductances varied within the range from ~1 to 30 nS. Semistable conductances were almost always observed until a successful pore abruptly expanded into the *T* stage, with conductances on the order of 1,000 nS (see Fig. 2). Typically, successful pores reached higher conductances than flickering pores: the maximal conductances reached by the transient pores (Fig. 9 *C*, $g_{f,max}$, *thick solid line*) were less than those attained by successful ones ($g_{s,max}$, *thin solid line*). Half of the transient pores never exceeded 3 nS; half of the successful pores remained <10 nS (Fig. 9 *C, thin solid line*).[2]

The distribution of maximal conductances of successful pores within the semistable stage (Fig. 9 *C, thin solid line*) was identical to the distribution of conductances from which these pores rapidly and fully enlarged (Fig. 9 *C*, $g_{S\text{-}T}$, *dotted line*). This implies that pores tended to fully dilate from the maximal conductances reached within the semistable stage. In contrast, transient pore closings tended to occur from minimal conductance levels (Figs. 6 and 7). In other words, while both successful and transient pores evolve from similar conductances, the larger the conductance the more likely it is that the pore will fully open.

DISCUSSION

The Fast Enlargement and Contraction of Transient Fusion Pore

The majority of fusion pores enlarged soon after formation, as conductances were increasing by the time they could be measured (Figs. 5 and 7 *A*). For a small frac-

2. Although, statistically, flickering pores underwent final closure from small conductances and did not enlarge as much as successful ones, some flickering pores reached and even closed from higher conductances than the maximum conductance attained by some successful pores.

tion of pores, we observed conductances that paused, for several ms, at intermediate values before increasing to a few nS (Fig. 5, *E* and *F*). These intermediate conductances, ~0.5 nS, were close to the values fusion pores fluctuate around for HAb2-erythrocyte fusion (Spruce et al., 1989; Zimmerberg et al., 1994) and for mast cell exocytosis (Spruce, Breckenridge, Lee, and Almers, 1990) before further pore expansion. We therefore envision that the nascent fusion pore between HA-expressing cells and the planar bilayer is small, ~0.5 nS or less, but rapidly (usually <4 ms) dilates to a larger semistable structure. Rapid enlargement is probably caused by the tension of the bilayer, on the order of 2 dyne/cm (Needham and Haydon, 1983), pulling on the pore. This fast growth is probably the reason pores are typically seen to be larger (1-4 nS) in HAb2 cell-planar bilayer fusion than in HAb2 cell-erythrocyte fusion (Spruce et al., 1989, 1991; Zimmerberg et al., 1994).

The transient fusion pore could be conceptualized in two ways. It could effectively function as a two-dimensional hole (e.g., disk) within a single bilayer that forms after two membranes hemifuse (Liberman and Nenashev, 1972; Neher, 1974; Chernomordik, Melikyan, and Chizmadzhev, 1987; Kemble, Danieli, and White, 1994) or it could be a tube-like structure that connects the two formerly distinct membranes, in which case the third dimension would assume importance. In the former case, the conductance would change with only pore diameter varying: for the latter, both pore length and diameter could vary.

If fusion pores were functionally two-dimensional objects, material from both monolayers of the cell membrane would be pulled into the planar bilayer by tension. Lipids from the cell would therefore have to pass through the highly curved region connecting the two membranes.[3] If the intrinsic radii of curvatures of some of the cell lipids were energetically unfavorable in the curved region, the force resulting from the unfavorable lipids within the bend could cause pore closing (Kozlov, Leikin, Chernomordik, Markin, and Chizmadzhev, 1989; Nanavati et al., 1992). On the other hand, if pores were tube shaped and elongated to the point where their lengths were greater than their diameters, bilayer tension would cause such pores to collapse (Melikyan, Kozlov, Chernomordik, and Markin, 1984). In this case, the slow conductance decrease observed before closing would be due to lengthening of the pore. The collapse of the tube would account for the fast final closing. In either conception, the tension of the bilayer is responsible for pore closings and provides a rational basis for why flickering is the rule in the cell-bilayer system (Melikyan et al., 1995) but infrequent in cellular systems with lower membrane tension (Zimmerberg et al., 1987; Spruce et al., 1990, 1991; Monck, Alvarez de Toledo, and Fernandez, 1990; Zimmerberg et al., 1994).

Evolution of Semistable Open Fusion Pores

We conjecture that the fate of pores exhibiting semistable conductances remains stochastic, always with possibilities either to close or to fully open, but more likely

3. It has been inferred that in mast cells lipid moves quickly from plasma to granule membranes connected by flickering fusion pores with conductances of a few nS (Monck et al., 1990). For fusion pores connecting HA-expressing cells to red blood cells, lipid does not move for conductances below ~0.5 nS, but moves unhindered when pores are on the order of nS (Tse et al., 1993; Zimmerberg et al., 1994). In the cell-bilayer system, nS conductances are attained rapidly.

to close from low conductances than from high conductances where they are prone to abruptly dilate to a diameter of microns. The probability that pores close or completely open would therefore be modulated as their dimensions, reflected in conductances, fluctuate. The conductance trajectories were virtually independent of HA density. Therefore, the growth of pores probably does not depend on accumulating HA trimers into their walls (Melikyan et al., 1995). We suggest that the evolution of pores was regulated by mechanical forces determined by mainly bending and surface tensions of the membranes defining the pores.

The notion that membrane mechanics governs dynamics of pores is intuitively appealing because pores with semistable conductances are relatively large. A conductance of 2 nS corresponds to a pore diameter of ~7 nm (for a three-dimensional pore), an order of magnitude greater than the diameter of a lipid molecule. The larger the pore the less one would expect the dynamics to be controlled by fusion-inducing proteins. For fusion pores of mast cell secretion (Curran et al., 1993) and for pores within single membranes induced to breakdown by excessive tension or electrical fields, semistable conductances also occur after a fast rise (Oberhauser and Fernandez, 1993). The very existence of semistable conductances suggests that pores reside in local energetic minima for extended times. The generality of the phenomenon strengthens the conjecture that membrane mechanics controls the trajectories of fusion pores.

Transient and Successful Open Pores Are Similar

Experimental evidence supports the notion that transient and securely open pores are initially identical structures: first, the initial conductances of transient and successful pores were identical (Fig. 9 *A*). Second, transient and successful pores exhibited similar initial rates of increase of conductance (Fig. 9 *B*).

The conductance profiles of transient and successful pores can be strikingly similar (Fig. 10). While open, this transient pore (*solid line*) was virtually indistinguishable from that of the successful pore (*open circles*) that followed it in the same experiment. Many examples of this near identity in conductance patterns were observed. The lifetime of the successful pore was longer than that of the transient pore (Fig. 10), in agreement with the finding that the open times of transient pores

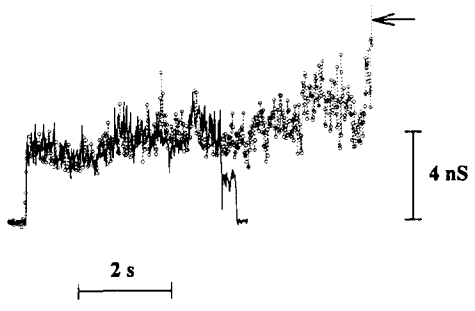

FIGURE 10. Conductance trajectories of transient and successful pores are similar. For the experiment shown, this was the last transient pore observed (*solid line*) before a successful pore (*open circles connected by dotted lines*) one. In this case, the two conductance trajectories (aligned at opening) were very alike overall until the transient pore closed. The successful pore fully enlarged (*arrow*) from the maximal conductance attained during the semistable stage. For visual clarity, pore conductance points of both pores were decimated (to 10 ms/pt).

were spread over shorter times than were the open times of successful pores (Melikyan et al., 1995).

We propose that transient and successful pores originate from the same fundamental structure, the small pore. Small pores enlarge with varied time courses to semistable sizes. Once semistable, pores can close or fully open. Membrane mechanics sets the energetics of a pore which in turn determines the probabilities of a pore's stochastic path. For conductances below ≈5 nS, the probability that a pore closes is greater than the probability to fully enlarge. This leads to multiple flickering and shorter lifetimes for transient open than for successful pores.

We thank Dr. Judith M. White for providing us with the HAb2 and GP4f cells and Dr. Leonid Chernomordik for critically reading the manuscript.

Supported by National Institutes of Health GM 27367.

Original version received 21 November 1994 and accepted version received 1 June 1995.

REFERENCES

Chernomordik, L. V., G. B. Melikyan, and Yu. 1994. A. Chizmadzhev. 1987. Biomembrane fusion: a new concept derived from model studies using two interacting planar lipid bilayers. *Biochimica et Biophysica Acta.* 906:309–352.

Curran, M., F. S. Cohen, D. E. Chandler, P. J. Munson, and J. Zimmerberg. 1993. Exocytotic fusion pores exhibit semi-stable states. *Journal of Membrane Biology.* 133:61–75.

Donnelly, D. F. 1994. A novel method for rapid measurement of membrane resistance, capacitance, and access resistance. *Biophysical Journal.* 66:873–877.

Ellens, H., J. Bentz, D. Mason, F. Zhang, and J. M. White. 1990. Fusion of influenza hemagglutinin-expressing fibroblasts with glycoprotein-bearing liposomes: role of hemagglutinin surface density. *Biochemistry.* 29:9697–9707.

Joshi, C., and J. M. Fernandez. 1988. Capacitance measurements. An analysis of the phase detector technique used to study exocytosis and endocytosis. *Biophysical Journal.* 53:885–892.

Kemble, G. W., T. Danieli, and J. M. White. 1994. Lipid-anchored influenza hemagglutinin promotes hemifusion, not complete fusion. *Cell.* 76:383–391.

Kozlov, M. M., S. L. Leikin, L. V. Chernomordik, V.S. Markin, and Yu. A. Chizmadzhev. 1989. Stalk mechanism of membrane fusion. *European Biophysical Journal.* 17:121–129.

Liberman, E. A., and V. A. Nenashev. 1972. Fusion of bimolecular membranes as a model of cell contact. *Biofizika.* 17:1017–1023.

Lindau, M., and E. Neher. 1988. Patch-clamp techniques for time-resolved capacitance measurements in single cells. *Pflügers Archiv.* 411:137–146.

Melikyan, G. B., M. M. Kozlov, L. V. Chernomordik, and V. S. Markin. 1984. Fission of bilayer lipid tubes. *Biochimica et Biophysica Acta.* 776:169–175.

Melikyan, G. B., W. D. Niles, M. E. Peeples, and F. S. Cohen. 1993*a*. Influenza hemagglutinin-mediated fusion pores connecting cells to planar membranes: flickering to final expansion. *Journal of General Physiology.* 102:1131–1149.

Melikyan, G. B., W. D. Niles, and F. S. Cohen. 1993*b*. Influenza virus hemagglutinin-induced cell-planar bilayer fusion: quantitative dissection of fusion pore kinetics into stages. *Journal of General Physiology.* 102:1151–1170.

Melikyan, G. B., W. D. Niles, and F. S. Cohen. 1995. The fusion kinetics of influenza hemagglutinin expressing cells to planar bilayer membranes is affected by HA density and host cell surface. *Journal*

of General Physiology. 106:783–802.

Monck, J. R., G. Alvarez de Toledo, and J. M. Fernandez. 1990. Tension in secretory granule membranes causes extensive membrane transfer through the exocytotic fusion pore. *Proceedings of the National Academy of Sciences, USA.* 87:7804–7808.

Monck, J. R., and J. M. Fernandez. 1992. The exocytotic fusion pore. *Journal of Cell Biology.* 119:1395–1404.

Nanavati, C., V. S. Markin, A. F. Oberhauser, and J. M. Fernandez. 1992. The exocytotic fusion pore modeled as a lipidic pore. *Biophysical Journal.* 63:1118–1132.

Needham, D., and D. A. Haydon. 1983. Tensions and free energies of formation of "solventless" lipid bilayers. *Biophysical Journal.* 41:251–257.

Neher, E. 1974. Asymmetric membranes resulting from the fusion of two black lipid bilayers. *Biochimica et Biophysica Acta.* 373:327–336.

Oberhauser, A., and J. M. Fernandez. 1993. Patch clamp studies of single intact secretory granules. *Biophysical Journal.* 65:1844–1852.

Plonsky, I., and J. Zimmerberg. 1994. Direct measurement of fusion pore conductance during virus-induced cell-cell fusion. *Biophysical Journal.* 66:A388. (Abstr.)

Pusch, M., and E. Neher. 1988. Rates of diffusional exchange between small cells and a measuring patch pipette. *Pflügers Archiv.* 411:204–211.

Rohlicek, V., and J. Rohlicek. 1993. Measurement of membrane capacitance and resistance of single cell at two frequencies. *Physiological Research.* 42:423–428.

Sambrook, J., L. Rodgers, J. M. White, and M.-J. Gething. 1985. Lines of BPV-transformed murine cells that constitutively express influenza virus hemagglutinin. *EMBO Journal.* 4:91–103.

Spruce, A. E., A. Iwata, J. M. White, and W. Almers. 1989. Patch clamp studies of single cell-fusion events mediated by a viral fusion protein. *Nature.* 342:555–558.

Spruce, A. E., L. J. Breckenridge, A. K. Lee, and W. Almers. 1990. Properties of the fusion pore that forms during exocytosis of mast cell secretory vesicle. *Neuron.* 4:643–654.

Spruce, A. E., A. Iwata, and W. Almers. 1991. The first milliseconds of the pore formed by a fusogenic viral envelope protein during membrane fusion. *Proceedings of the National Academy of Sciences, USA.* 88:3623–3627.

Tse, F. W., A. Iwata, and W. Almers. 1993. Membrane flux through the pore formed by a fusogenic viral envelope protein during cell fusion. *Journal of Cell Biology.* 121:543–552.

White, J. M. 1992. Membrane fusion. *Science.* 258:917–924.

White, J. M., A. Helenius, and M.-J. Gething. 1982. Haemagglutinin of influenza virus expressed from a cloned gene promotes membrane fusion. *Nature.* 300:658–659.

Zimmerberg, J., M. Curran, F. S. Cohen, and M. Brodwick. 1987. Simultaneous electrical and optical measurements show that membrane fusion precedes secretory granule swelling during exocytosis of beige mouse mast cells. *Proceedings of the National Academy of Sciences, USA.* 84:1585–1589.

Zimmerberg, J., S. S. Vogel, and L. V. Chernomordik. 1993. Mechanisms of membrane fusion. *Annual Review of Biophysics and Biomolecular Structure.* 22:433–466.

Zimmerberg, J., R. Blumenthal, D. P. Sarkar, M. Curran, and S. Morris. 1994. Restricted movement of lipid and aqueous dyes through the pore formed by influenza hemagglutinin during cell fusion. *Journal of Cell Biology.* 127:1885–1894.